24th INTERNATIONAL CONGRESS ON SOUND AND VIBRATION
23–27 July 2017, London

EFFECTS OF PORE-SIZE DISTRIBUTION ON SOUND ABSORPTION OF MATERIAL FABRICATED BY ADDITIVE MANUFACTURING

Xiaolin Wang and Hao Liang

Laboratory of Noise and Vibration Research, Institute of Acoustics, Chinese Academy of Sciences, Beijing 100190, China
email: wangxl@mail.ioa.ac.cn

For porous materials, it is widely acknowledged a proper pore-size distribution would enhance effective absorbing sound frequency bandwidth. If we can find such a distribution, it could have potentials for extending the range of low frequencies. However, there still are questions lacking satisfactory answers, such as how exactly various distributions would affect or how to make use of a distribution to improve sound absorption. One obstacle to answering these questions lies in the limitation of choices in a controlled pore-size distribution of realistic materials to verify a theory, if ever developed for such distribution. With the development of additive manufacturing, solutions are now opened up to remove this obstacle. In this paper, with samples fabricated by additive manufacturing, a theory developed on two-dimensional pore-size distributions is verified by experimental results. With corrections offered by experimental methods, including flow resistance measurement and three-dimensional micro-CT imaging, the experimental results agreed well with theoretical results. How to improve low frequency sound absorption by making use of pore-size distribution is also explored.
Keywords: sound absorption, pore-size distribution, additive manufacturing

1. Introduction

For porous materials, it is widely acknowledged a proper pore-size distribution would enhance effective absorbing sound frequency bandwidth. If we can find such a distribution, it could have potentials for extending the range of low frequencies. However, there still are questions lacking satisfactory answers, such as how exactly various distributions would affect or how to make use of a distribution to improve sound absorption. One obstacle to answering these questions lies in the limitation of choices in a controlled pore-size distribution of realistic materials to verify a theory, if ever developed for such distribution. With the development of additive manufacturing, solutions are now opened up to remove this obstacle.

It has long been noted among geophysicists a correlation between the permeability and the distribution of pore sizes in porous materials. McCann and McCann [1] noted effects of the pore-size distribution on compressional wave attenuation in water-saturated sediments. They proposed a solution by incorporating this distribution with Biot's theory [2], especially for the permeability. Later, Yamamoto and Turgut [3] proposed corrected mathematical expressions for the permeability as well as the viscous correction factor used in the Biot theory. They concluded that acoustic properties are independent of the pore-size distribution at the low- and high-frequency limits but strongly dependent on the distribution in the intermediate frequency range. Horoshenkov *et al* [4] then derived expressions for complex density and compressibility based on distribution-dependent expressions for the viscosity correction function and the flow resistivity. Practical two-point Padé approximants for the correction function were then derived. Following this work, there have been a num-

ber of articles dealing with various materials, such as granular materials with log-normal distributions [5], double-porosity materials with multiscale distributions [6] and mixtures of hemp particles with pore-size distributions related to particle shape and particle-size distributions [7]. Instead of incorporating the pore-size distribution with the viscosity correction factor, Tarnow developed a model [8] for airflow resistivity of fibrous materials with randomly placed parallel cylinders, each lies in a Voronoi polygon, which is then replaced by an effective circular cell. In addition to theoretical developments and applications, there are also experimental observations on sound absorption affected by pore-size distributions in materials such as phenolic foams [9], titanium fibres [10], porous polydimethylsiloxane and cement composites [11].

Following Tarnow's line of dealing with pore-size distribution, Wang and Lu [12] then assumed in a model that the mean complex density and compressibility of a two-dimensional Voronoi-distribution material could follow a similar treatment. Although calculations were conducted to examine effects of that distribution, this model was not experimentally verified due to difficulties of fabricating proper samples at the time of publication. With the development of additive manufacturing, we are now able to fabricate. In our current paper, with samples fabricated by additive manufacturing, this model developed on two-dimensional pore-size distributions is compared with experiments. With corrections offered by experimental methods, including flow resistivity measurement and three-dimensional micro-CT imaging, the experimental results agreed well with theoretical results. How to improve low frequency sound absorption by making use of pore-size distribution is also explored.

2. Model of Sound Absorption

For a layer of acoustic material with thickness L_s having characteristic acoustic impedance Z_p and propagation constant k_p, its sound absorption coefficient α at the surface with specific acoustic impedance Z_s and normal to the impinging sound wave is

$$\alpha = 1 - \left| \frac{Z_s - Z_0}{Z_s + Z_0} \right|^2 . \tag{1}$$

where $Z_0 = \rho_0 c_0$ is the characteristic impedance in free air. The specific impedance Z_s can be obtained if the material is mounted on a hard termination

$$Z_s = Z_p \coth(k_p L_s) . \tag{2}$$

The characteristic impedance Z_p and propagation constant k_p are two fundamental characteristics of material describing sound propagation. These two can also be expressed in terms of another set of material characteristics, i.e. the complex density and compressibility of the material, ρ and C, respectively, while the angular frequency of sound is ω and $i = \sqrt{-1}$:

$$Z_p = \sqrt{\rho / C}, \qquad k_p = i\omega\sqrt{\rho C} . \tag{3}$$

Here for simplicity we consider a bulk medium comprising a group of rigid circular ducts with a distribution of radius r. These ducts are parallel to each other all along the propagation direction of the incident sound. If the distribution density function of duct cross-sectional areas is p_v , the mean radius of the ducts is r_v, $\bar{r} = r/r_V$, then the complex density and compressibility of the material are

$$\rho = \frac{q^2 \rho_0}{\Omega} \int_0^\infty \left[1 - \frac{2}{\sqrt{-i}\kappa\bar{r}} \frac{J_1(\sqrt{-i}\kappa\bar{r})}{J_0(\sqrt{-i}\kappa\bar{r})} \right]^{-1} p_V 2\pi\bar{r} d\bar{r} . \tag{4}$$

$$C = \frac{\Omega}{\gamma_0 P_0} \left[1 + (\gamma_0 - 1) \int_0^\infty \frac{2J_1(\sqrt{-iN_{pr}}\kappa\bar{r})}{J_0(\sqrt{-iN_{pr}}\kappa\bar{r})} \frac{p_V 2\pi\bar{r} d\bar{r}}{\sqrt{-iN_{pr}}\kappa\bar{r}} \right] . \tag{5}$$

where q is the tortuosity, Ω is the density; P_0, ρ_0, and γ_0 are the pressure, density and specific heat ratio of air respectively; N_{pr} is the Prandtl number, $\kappa = \sqrt{\omega\rho_0/\mu}r_V$ is the acoustic Reynolds number with μ the dynamic viscosity; J_0 and J_1 are the Bessel functions of the first kind.

3. Materials and Methods

In order to verify Eqs. (4) and (5), two samples were fabricated by 3D printing. Our main concerns here are effects of pore-size distribution, the design of this fabrication therefore are made on the following three conditions:

- In order to apply the model in Section 2, fabricated samples need to be relatively rigid. Here we chose PVC. Each duct is a straight cylinder with its axis along the direction of sound propagation but perpendicular to the front of the sample facing the sound source.
- In order to concentrate on pore-size distribution, parameters of samples such as the mean radius r_v , sample thickness L_s, porosity Ω were kept constant. Here we chose r_v = 500μm, L_s= 10mm, Ω = 0.5. In order to achieve a relatively high resolution, a StrataSys printer with resolution of 16ppi was selected for 3D printing.
- Regarding pore-size distribution, for a specific probability density function, we are concerned with how much the peak of the function is skewed from its mean radius. Two samples S1 and S2 were then fabricated with roughly the same distribution width, but one with a normal distribution the other with a skewed peak, shown in Figs. 1 and 2.

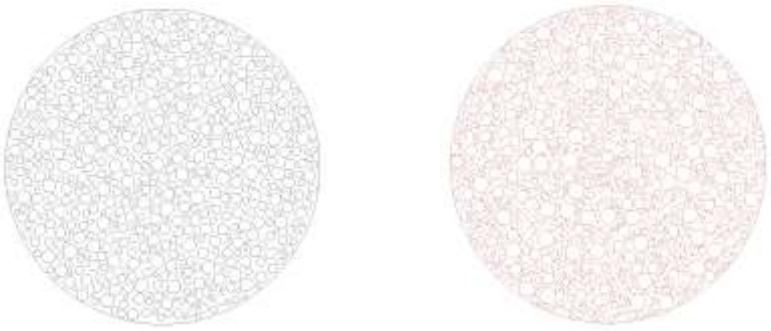

Figure 1: Designs of samples showing their cross-sectional features, S1 left and S2 right.

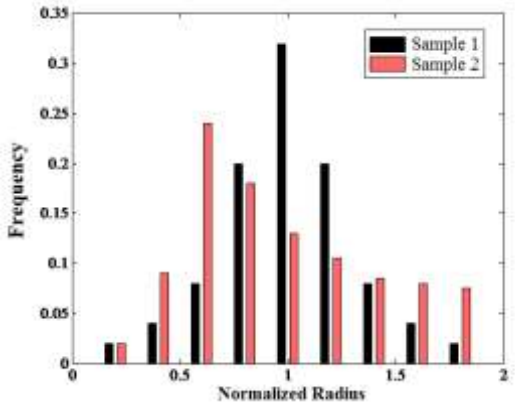

Figure 2: Probability distributions of sample S1 and S2. Normalized radius $\bar{\boldsymbol{r}} = \boldsymbol{r}/\boldsymbol{r_V}$.

Our experience shows that at this stage of 3D printing, for the purpose of acoustical test at least, there is no guarantee that the final manufactured samples would be ready for acoustic calculation if just based on designed data. There are obvious discrepancies, which could even reach a relative error of at least 30%, mostly at the high frequency end. A 3D micro-CT imaging has proved to be a useful tool for counting pore-size distributions which can rectify and reduce this error.

A SCANCO medical μCT50 micro-CT scanner was used for refined counting of pore-size distribution. It was found the measured mean radii of both samples are about 370-390 μm, the measured porosities are about 0.33-0.36, measured airflow resistivities are about 2600 Pa s/m^2. Between the two samples, their mean radii, porosities and resistivities are almost the same to each other, all within the range of 10% error. Our requirements of fabrication for the study of pore-size distribution are thus satisfied, Figs. 3 and 4 are scanned images and comparisons between measured and designed distributions.

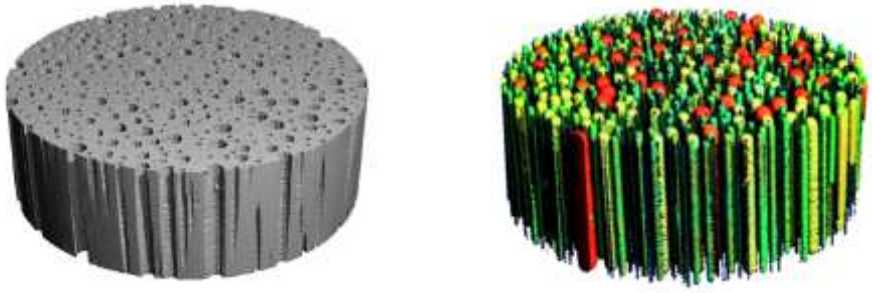

Figure 3: Reconstructed image of sample S2 and its coloured image showing pore-size distribution.

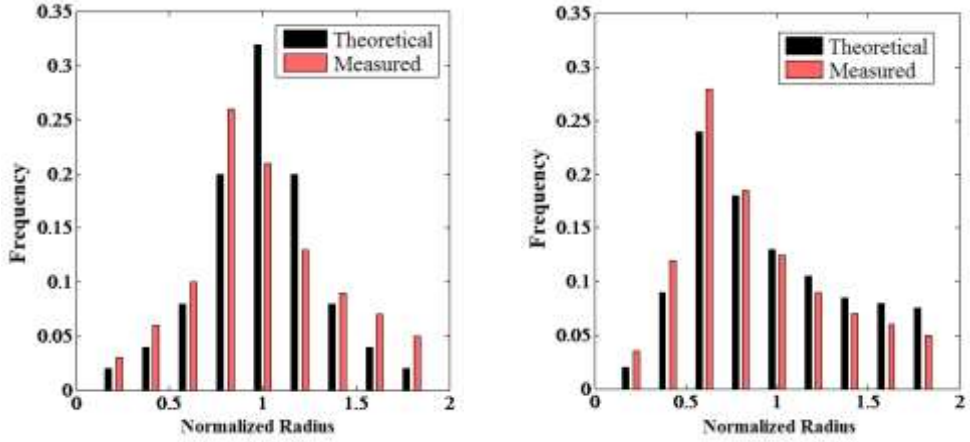

Figure 4: Designed and measured distributions of samples S1 and S2. Normalized radius $\bar{\boldsymbol{r}} = \boldsymbol{r}/\boldsymbol{r_V}$.

4. Results and Discussions

Sound absorption measurements were conducted on a B&K Type 4206 impedance tube with samples either mounted on a hard termination or with an air cavity behind. Figures 5 and 6 are plots of sound absorption measurements of the two samples. Note that there are still some discrepancies at the high frequency end. These may be caused by the surface roughness inside fabricated capillary ducts, nevertheless theoretical results from the proposed mode fit with experimental results.

After verification, we then look at how different distributions affect sound absorption by taking examples of three typical distributions: the uniform-, normal- and Γ-distributions as follows:

$$p(\bar{r}) = r_V / D = 1/\mathrm{w}\,.$$

$$p(\bar{r}) = \frac{1}{\sqrt{2\pi}\sigma}\exp\left[-\frac{(\bar{\mathrm{r}}-1)^2}{2\sigma^2}\right]. \tag{6}$$

$$p(\bar{r}) = \frac{a^a}{r_V\Gamma(a)}\bar{r}^{a-1}\mathrm{e}^{-a\bar{r}}\,.$$

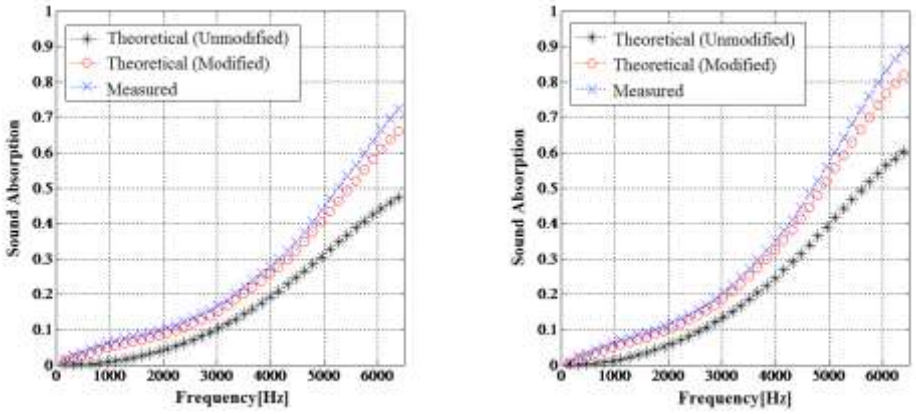

Figure 5: Experimental and theoretical results after CT-scanning corrections, S1 left and S2 right.

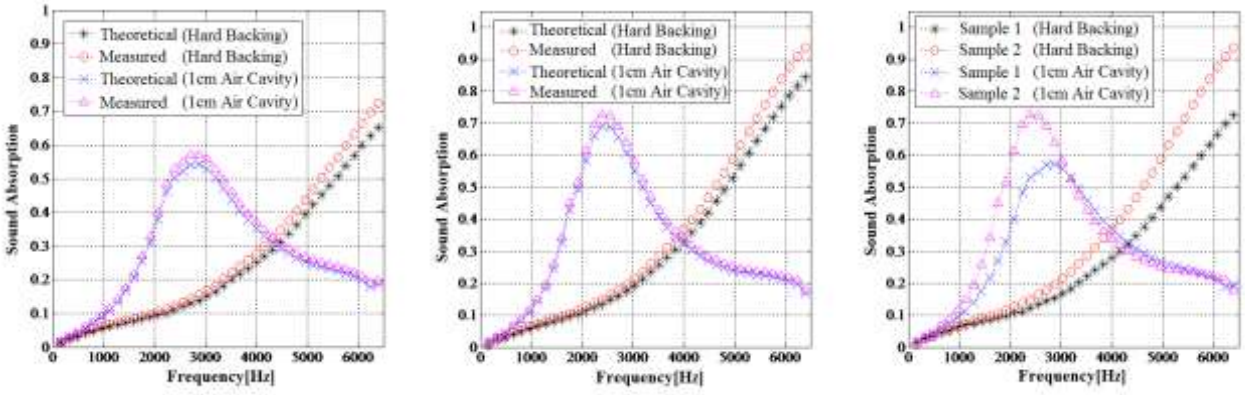

(a) (b) (c)

Figure 6: Comparisons between theoretical and experimental results, (a) S1, (b) S2; Comparisons between samples (c) S1 and S2.

where w is the normalized range of radius, i.e. difference between the maximum and minimum normalized radius, a measure of the width of the distribution. The parameter σ is also normalized by the mean radius, as well a measure of the distribution width. The parameter a is a measure of the skewness of the distribution peak from the mean radius. Figure 7 shows effects of these parameters on the distribution, while Fig. 8 shows effects of these parameters on the sound absorption.

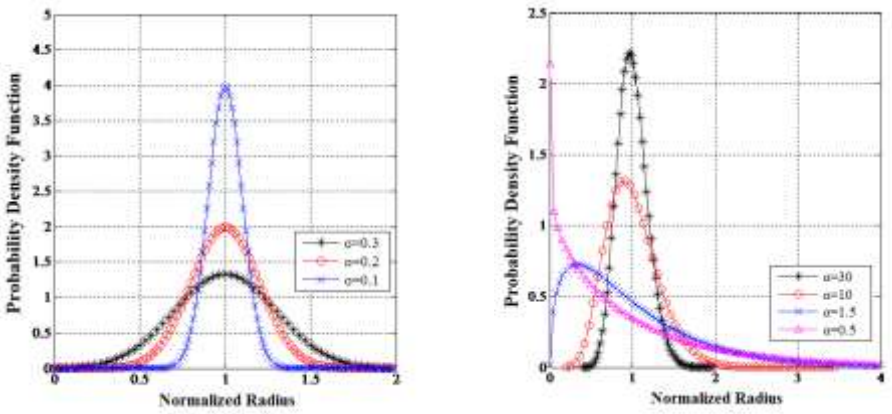

Figure 7: The normal-distribution and the Γ-distribution.

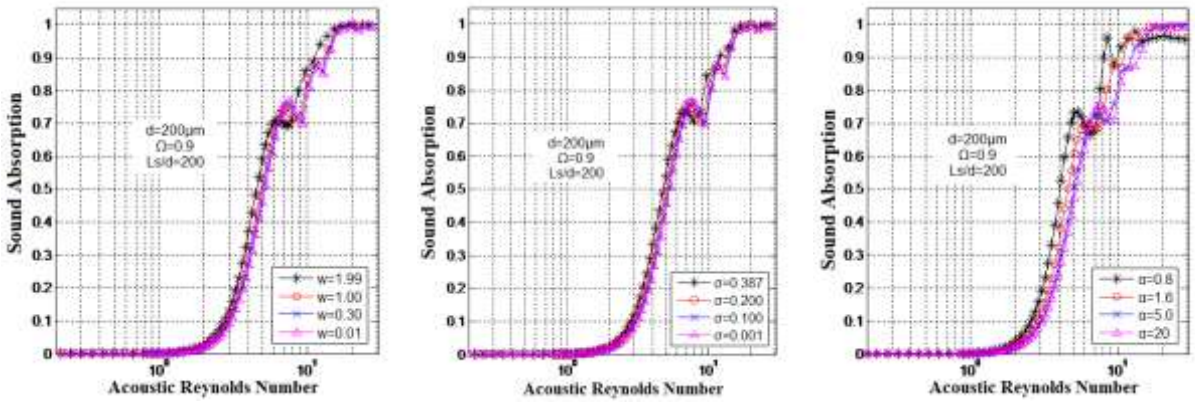

Figure 8: The uniform-, normal and Γ-distributions.

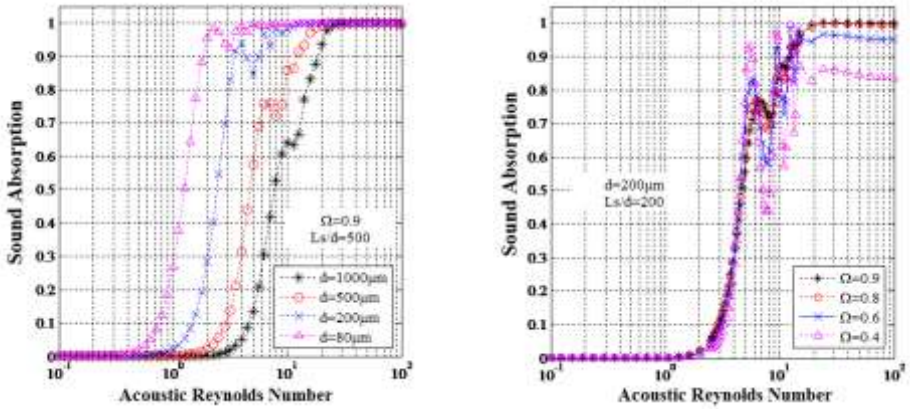

Figure 9: Sound absorption affected by porosity and single-pore-size distribution

Next, we look at effects of porosity and distribution of a single pore-size on sound absorption in Fig. 9. It can be seen how much a chosen pore-size could affect low frequency absorption, while a lower porosity could significantly increase the low frequency absorption peak and slightly shift the peak frequency. However, that increase of the peak is achieved at the cost of a deepened trough next to the peak. It appears that the wider the distribution width, the wider the frequency range of high absorption, especially extended towards the low frequency end. The skewness of the peak away from the mean radius tends to increase sound absorption as well.

5. Conclusion

In this paper, sound absorption of porous materials with two-dimensional pore-size distribution has been examined, with the help of additive manufacturing for fabricating samples and three-dimensional micro-CT imaging for realistic pore-size counting. In order to concentrate on effects due to pore-size distribution, particularly the skewness of the distribution peak, two samples were fabricated with roughly the same mean radius, distribution width, porosity, thickness and airflow resistivity. Experimental results agreed well with the theoretical results made from a previously proposed model. Further calculations were followed for four types of distributions, i.e., a single-pore-size, the uniform-, normal- and Γ-distributions. It is noted in order to enhance sound absorption at low frequencies, it might be a good idea to decrease the porosity, but this probably will lead to a deepened trough in the absorption next to the peak frequency. There needs to be a balance between the absorption at low frequencies and the overall absorption in a wider frequency range. For sound absorption, the mean radius decides where a low frequency range is likely to be affected, while the distribution width slightly affects the frequency bandwidth. Finally, results have shown that if the peak is skewed to the smaller radius side, it is likely to increase sound absorption in the whole concerned frequency range, while slightly decreasing the first absorption peak frequency.

ACKNOWLEDGEMENTS

The authors gratefully acknowledge the support from the National Natural Science Foundation of China (No.11574344, No.11404369) and the National Basic Research Program of China (No 2011CB610302, No 2012CB720204). The first author also would like to thank Zhehao Huang for adapting figures to be included in this paper.

REFERENCES

1 McCann, C. and McCann, D. M., *Geophysics*, **50**(8), 1311-1317, (1985).

2 Biot, M. A., *The Journal of the Acoustical Society of America*, **28**(2), 179-191, (1956).

3 Yamamoto, T. and Turgut, A., *The Journal of the Acoustical Society of America*, **83**(5), 1744-1751, (1988).

4 Horoshenkov, K. V., Attenborough, K. and Chandler-Wilde, S. N., *The Journal of the Acoustical Society of America*, **104**(3), 1198-1209, (1998).

5 Horoshenkov, K. V. and Swift, J., *The Journal of the Acoustical Society of America*, **110**(5), 2371-2318, (2001).

6 Pispola, G., Horoshenkov, K. V. and Khan, A., *The Journal of the Acoustical Society of America*, **121**(2), 961-966, (2007).

7 Glé, P., Gourdon, E., Amaud, A., Horoshenkov, K. V. and Khan, A., *The Journal of the Acoustical Society of America*, **134**(6), 4698-4709, (2013).

8 Tarnow, V., *The Journal of the Acoustical Society of America*, **100**(6), 3706-3713, (1996).

9 Gong, R., Xu, Q., Chu, Y., Gu, X., Ma, J. and Li, R., *RSC Advances*, **5**, 68003-68013, (2015).

10 Liu, S. F., Tang, H. P., Liu, B., Ao, Q. B., Zhang, Z. H. and Liu, Q. M., *Journal of Sichuan University (Natural Science Edition)(in Chinese)*, **51**(1), 160-164, (2014).

11 Rutkevicius, M., Mehl, G. H., Paunov, V. N. and Qin, Q., *Journal of Materials Research*, **28**(17), 2409-2414, (2013).

12 Wang, X. L. and Lu, T. J., *The Journal of the Acoustical Society of America*, **106**(2), 756-765, (1999).